THE EFFECT OF MACH NUMBER ON LP TURBINE BLADE WAKE INTERACTION

M. Vera, H. P. Hodson
Whittle Laboratory
University of Cambridge, UK

R. Vazquez
ITP, Industria de Turbo Propulsores
Madrid, SPAIN

Abstract

The techniques employed in high speed linear cascade testing to simulate the effect of unsteadiness are presented and compared with low speed counterparts. Results are obtained from a high speed cascade and a low speed cascade. Both are models of an existing (conventional) low pressure turbine blade. They are compared under steady and unsteady flow conditions. The results show that the same quantitative values of losses are obtained, proving the validity of the low speed approach for profiles with an exit Mach number of the order of 0.64. The range of validity of the conclusions is extended by reference to a profile designed using current low pressure turbine design practice. Wake traverses using pneumatic probes reveal that the unsteadiness reduced the profile losses up to Mach numbers of 0.9

1. Introduction

The development of the low pressure turbine (LPT) has reached a stage where rises in efficiency are difficult to obtain. Furthermore, the LPT could represent one third of the total engine weight. Therefore, one of the current trends that designers have adopted is to improve the overall performance of the LPT by reducing its weight. This new philosophy leads to fewer blades each of which carries a greater aerodynamic load.

The LPT operates at the lowest Reynolds number in the whole engine. This means that the development of the boundary layers will be determined by the transition from laminar to turbulent flow. Increasing the aerodynamic load increases the diffusion on the rear part of the blade and thus the risk of separation. In fact, the resulting blade usually features a large separation bubble in steady flow conditions. This can be partially or totally suppressed by transition to turbulent flow being

caused by the wakes coming from an upstream row of blades. Due to the ability of the wakes shed by an upstream row to promote transition in the neighborhood of separation, the study of wake-boundary interactions is of primary interest in the LPT environment. The large aspect ratio of the LPT blades (typically between 3 and 7) makes them appropriate for linear cascade testing.

Previous studies on wake induced transition phenomena for high speed flows have been carried out by others researchers (Brunner et. al, 2000 and Coton et. al, 2002) but still, very little is known about the topic. This fact together with the current limitations of the CFD tools (Vilmin et at, 2003) suggests that experimental studies of blade-wake interaction phenomena in high speed flows are needed. Even though the experimental techniques used in high speed testing are conceptually the same as those used in low speed, the problems encountered tend to be magnified at high speed. In addition, new challenges arise. Therefore, we should question when it is worth doing high speed cascade testing.

This paper aims to answer this question. It examines the extent to which the results from the low speed approach are meaningful. This paper follows previous comparisons between high speed and low speed testing, (Wisler, 1984), (Hodson and Dominy, 1993), by presenting a comparison between high speed and low speed testing of LPT linear cascades. In the main part of this paper, two profiles are compared. These profiles are not identical but they both are intended to model an existing LPT blade in the cascade environment at low speed or at high speed. Facilities and instrumentation will also be compared. Finally, results from a modern LPT blade will be presented to demonstrate the extent to which the conclusions are valid. To conclude, the behavior of this blade is presented up to exit Mach numbers of 0.9.

2. DESIGN PROCESS

In using high speed cascades, few compromises are needed to achieve a model of the real blade in the turbomachine. Indeed, true similarity can be obtained sometimes. In the case of low speed cascades, more compromises are required and the shape of the resulting low speed blade usually differs greatly from the real blade to be modelled. Typical sizes of the resulting LPT blades for both high and low speed cascade testing at the Whittle laboratory are shown in Table 1.

2.1 Choosing the bars

To achieve a realistic simulation of the rotor-stator interaction, several similarity parameters must be correctly matched. The method used to

choose the size and the pitch of the bars is the same in low and high speed cascade testing and it is presented below. Only by following this procedure is a good simulation of the rotor-stator interaction situation achieved.

To reproduce the kinematics of the wake-blade interaction, the flow angle β_1 in the bar relative frame of reference, is matched to that of the upstream bladerow in the LPT. The relative and absolute inlet flow angles and the inlet axial velocity to the cascade, V_{x1}, then give the speed of the bars, U, from the velocity triangles at the inlet of the cascade.

The reduced frequency of the machine not only sets the ratio of the convection time scale to the wake passing time scale, but it also sets the ratio of the viscous diffusion time scale to the wake passing time scale. Therefore, it must be matched if a realistic rotor-stator interaction is to be achieved. The reduced frequency, F, and the bar passing frequency, f, are related according to the expression

$$F \equiv fC/V_2 = U/s_{bar} \cdot C/V_2 \propto f \cdot x/U \tag{1}$$

where C is the chord of the airfoil. Equation 1 provides the bar passing frequency and the pitch of the bars, s_{bar}. The reduced frequency is defined in terms of the exit velocity of the cascade, V_2. This is because the most important wake-blade interactions tend to occur in the latter half of the blade passage. Typical values of the bar passing frequencies for high speed and low speed cascades are given in Table 1.

Pfeil and Eifler (1976) showed that the structure of the far wake of an airfoil and that of a cylindrical body of the same drag is almost the same. If an estimation of the stagnation pressure losses of the blade row to be simulated is known, Y_p, the diameter of the bars, d, can be obtained according to

$$Y_p = d \cdot C_d/(s_{bar} \cdot Cos\beta_1) \tag{2}$$

which is exact for low speed flows. An estimation of the drag coefficient of the bars, C_d, at the relative conditions that Y_p represents, must be known. Typical dimensions of the resulting diameters of the bars are given in Table 1. These values are of the same order than the trailing edge thickness of the upstream blade row.

Once all the previous values are fixed, the ratio between the pitch of the cascade, s, and the pitch of the bars is known. Also, the flow coefficient of the bars, ϕ, is given by

$$\phi = V_{x1}/U \tag{3}$$

and this is fixed by the inlet angle in the cascade frame of reference.

	High speed	Low speed
Chord (mm)	50	200
Bar diameter (mm)	0.41	2
Bar passing frequency	3 kHz	200 Hz

Table 1. Typical dimensions of blades and bars in low speed and high speed cascades at the Whittle laboratory.

3. TEST FACILITIES AND INSTRUMENTATION

For the present work, two linear cascade facilities have been used. The description of the low speed passing bar linear cascade facility was previously documented by Banieghbal et. al, (1995). It is the aim of this paper to describe the high speed rotating bar linear cascade facility and to compare it with its low speed counterpart.

3.1 Transonic cascade facility

The high speed experiments were carried out in the transonic cascade facility at the Whittle laboratory. This is a continuous flow, closed-circuit variable density wind tunnel where Reynolds and Mach number can be fixed independently. Two vacuum pumps, working in parallel, are used to achieve sub-atmospheric pressures. A compressor is used to control the pressure ratio and thus the Mach number of the flow within the circuit. To control the humidity of the air, some of the air is passed through a dryer. The temperature variation can be limited by adjusting the cooling system. Before entering the cascade, the air passes through a honeycomb and screen in order to filter the air and to break up any large scale structures that may exist in the flow. At the entry to the cascade, the flow is accelerated in a convergent nozzle. At the exit, it is discharged into the large exit plenum that contains the test section.

3.2 Wake generators

The presence of the wakes shed from an upstream blade row is simulated using a wake generator. At the Whittle laboratory, the low speed cascades, the wake generator consists of bars fitted between two belts placed on either side of the side walls. The wake generator is driven by a motor by means of mechanism of belts and pulleys and provides linear motion to the bars.

In high-speed flows, the matching of similarity parameters demands a higher speed from the bars. For mechanical reasons this cannot be achieved with the type of bar passing wake generator typical of low speed rigs. Instead, the high speed bar wake generator consists of a number of

metal bars equally spaced at the outer periphery of a disk that rotates in a plane parallel to the leading edge plane of the cascade. In this way the circumferential speed of the bars can be increased to the levels that are required in the cascade experiments. A cover encloses the rotating disk and bar assembly thus creating a sealed chamber containing the bars. This sealed cavity is needed to prevent the leakage that would occur if the cavity were opened to the plenum, i.e., to exit conditions. Low speed cascade testing tends to suffer from this sort of leakage. Therefore, controlling the inlet periodicity is easier in high speed due to the sealed chamber that contains the bars. The cover has a rectangular opening aligned with the exit of the convergent nozzle over which the cascade is

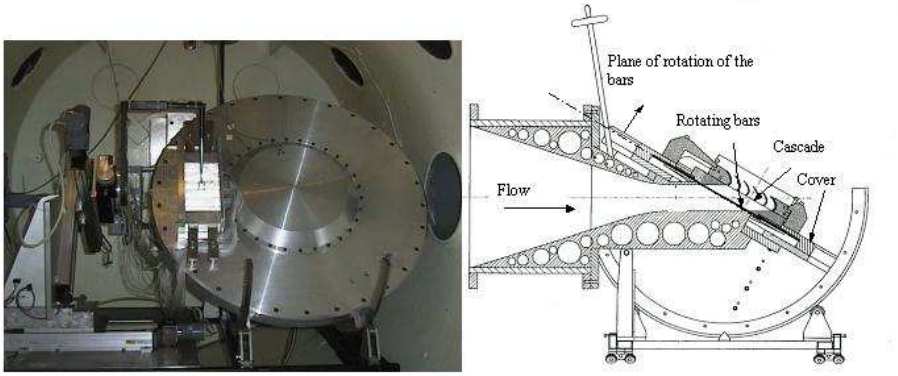

Figure 1. High speed rotating bar rig, frontal view (left) and cross section (right)

The bars move across the front of the cascade, thus simulating the upstream blade row. In the high speed rotating bar rig the bars are made of hypodermic tube. They are fitted at the outer periphery of the rotating disk. When the bars cross the test section, they are subjected to a transverse aerodynamic loading. This loading deflects the bars and thus limits their performance. The deflection, δ, must be smaller than the distance between the bars and the cover [1].

The bars are also subjected to an axial loading due to centrifugal effects. The axial tension tends to straighten the bars and thus reduces their deflection. The deflection is reduced, for a given diameter of the

[1]This distance is shorter than the axial gap between the bars and the leading edges of the cascade

bars, by placing a weight on the tip of the bars. Additionally, when the bars leave the test section, the aerodynamic loading ceases. This transient leads to forced vibrations of the bars. By placing the weight on the tip of the bars, these vibrations are also reduced. The maximum mass that can be used is given by the maximum strength of the material.

The above discussion shows how to avoid some the mechanical constraints limiting the performance of the bars. These limitations must be taken into consideration when fixing the scale of the cascade. Only in this way can a realistic simulation of the blade-wake interaction phenomena be achieved.

3.3 Instrumentation

The instrumentation for high speed measurements is conceptually the same as that used for low speed testing. This instrumentation is described by Banieghbal et. al, (1995). The differences between the acquisition of data in low speed and high speed flows are due to the different scales of the values to be measured. This influences the quality of the measurements by influencing the resolution of the output of the signal and the resolution of the characteristic time.

The response frequency of conventional hot films and hot wires is of the order of 25 to 50kHz. The scale of the boundary layers and the freestream velocity indicates that the lowest turbulent frequencies are expected to be of the order of 3kHz and 100kHz for the low speed and high speed blades respectively. Therefore, the lowest turbulent frequencies can be characterized only for low speed flows. Additionally, Table 1 presents the typical value of the bar passing frequency in high speed cascade testing. This is of the order of 3kHz. Thus, for a given the response frequency of the anemometers, a poorer resolution of the bar passing period is obtained for high speed cascades.

4. RESULTS

4.1 Inlet conditions to the cascade

The time mean conditions at inlet to the cascade are affected by the bars. These effects are due to the creation of entropy by the bars and work done by the component of the drag force of the bars in the direction of movement of the bars. In the ideal case, the time mean conditions at the inlet of the cascade can be measured by placing probes downstream of the bars. However, the distance between the bars and the leading edges of the cascade is usually small (25-50% of the chord). Therefore, access is difficult, especially in small scale, high speed cascades. Furthermore,

the flow is unsteady. This can result in false readings from conventional instrumentation. Also, due to the presence of the blades, the time-mean inlet stagnation conditions may not be pitchwise uniform in the unsteady flows (Hodson and Dawes, 1996). To avoid these problems, a calculation procedure is used to determine the (mixed out) conditions downstream of the bars.

A control volume representing the flow through the row of bars, in the relative frame of reference, is shown in figure 2. The drag force, D, represents the force produced by the bars on the fluid. It is taken to act against a direction averaged with both inlet an exit directions. This model is a modified version of the model proposed by Schulte and Hodson (1996). In their model an incompressible analysis of the same control volume is made, assuming that D acts in the same direction as the flow entering in the control volume. The validation of this method for incompressible flow can be found in Schulte (1995). The validation for compressible flow is presented below.

The drag coefficient of the bars, C_d, is defined by

$$C_d = D/(d \cdot (P_{00,rel} - P_{s0})) \tag{4}$$

and

$$tan\beta_m = (tan\beta_0 + tan\beta_1)/2 \tag{5}$$

defines the direction against which the drag force acts.

On surfaces S_b and S_d, periodic boundary conditions apply and no net flow crosses these surfaces. Flow enters the control volume with a uniform velocity through surface S_a and leaves the control volume through surface S_c. It is assumed that mixed out conditions are already reached at surface S_c. The continuity, momentum and energy equations

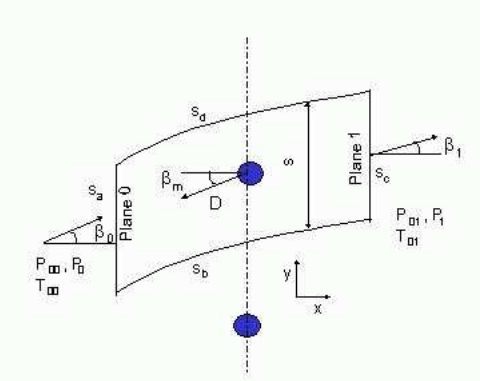

Figure 2. Control volume. Frame of reference fixed to the bars

form an implicit system of equations that have to be solved for each inlet condition.

The solution to the system of equations depends, amongst others, on the drag coefficient of the bars, C_d. The value of C_d depends on the conditions at plane 0. Therefore, in order to solve the system of equations, the value of C_d has to be known for the range of Reynolds numbers and Mach numbers found in the measurements.

For the determination of C_d, the drag force produced by the bars, D, must be known. To measure D, the wake of one single stationary bar was traversed. Knowing the drag force, the drag coefficient of the bar can be calculated using (4). The value of C_d was measured for the entire range of Reynolds and Mach numbers covered by the measurements. By knowing the value of C_d, the implicit system of equations can be solved for a given value of the conditions upstream the bars and flow angle. Thus, the mixed out conditions downstream the bars can be determined.

The calculation of the conditions downstream of the moving bars will be now validated with experimental results. The measurements were performed in the high speed rotating bar rig. The cascade was removed and a pneumatic probe was placed downstream of the bars. The probe was placed in the plane where the leading edges of the cascade would have been. The conditions upstream the bars corresponded to the design inlet conditions of the cascade.

Downstream of the bars, the probe was traversed in the pitchwise direction at three different spanwise positions. The measured upstream conditions are used to calculate the conditions downstream of the bars by means of the calculation procedure described above. A comparison between the downstream measurements and the calculated values is shown in figure 3. The abscissa represents the radius of the bars at each measurement point. This value is non-dimensionalised by the radius of the bars at 50% of the span and at a pitchwise position that would correspond to the centre of the cascade. The ordinate represents the reduction in stagnation pressure through the row of bars expressed as a fraction of the equivalent exit dynamic pressure of the datum high speed cascade at design conditions. At $r/r_{50\%span}$ equal to 1, the differences between prediction and experiments are less than 0.1% of the cascade exit dynamic pressure. A good agreement between the calculation procedure and the measurements is found, thus validating the method.

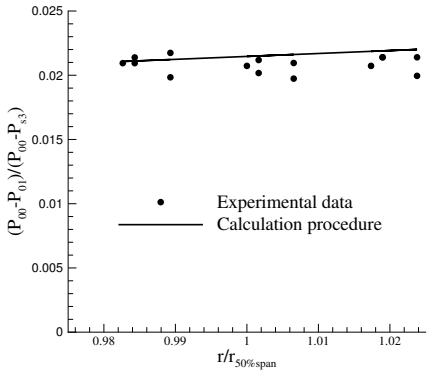

Figure 3. Comparison of experimental data and calculations for the loss of stagnation pressure across the bars at design conditions of the cascade, $Re_3 = 1.9 \times 10^5, Ma_3 = 0.64$.

4.2 Datum Profiles

In this section, the results from a high speed and a low speed cascade both being the model of an existing LPT blade are compared for steady and unsteady flow conditions. The comparison includes Mach number (velocity) distributions, profile loss measurements and surface mounted hot-film measurements.

4.2.1 Mach number distribution. Figure 4 shows a plot of the distribution of isentropic Mach number for the high speed and low speed cascades under steady flow conditions. The values are non-dimensionalised by the exit isentropic Mach number. The suction peak occurs at 55% of the suction surface length for both blades. The ratio of the maximum surface isentropic Mach number to the exit isentropic Mach number is about 1.15 for both profiles. The flow separates at about 75% of the suction surface length for both cases. Differences are seen in the region covered by the suction side separation bubble. For a similar length of bubble in both blades, the acceleration due to the blockage of the bubble is bigger in the case of the high speed profile. This is due to compressibility effects. For both profiles, the flow is attached to the blade surface at the trailing edge.

According to Banieghbal et. al, 1995, a pressure side separation bubble occurs on both blades. The Mach number distributions show differences in this region. These could be due to errors in the measurements of the very low velocities associated to the bubble on the low speed pro-

file.The length of the bubble is the same for t he high speed and the low speed profile. The bubble extends up to 50% of the pressure surface length. From this position, the flow accelerates towards the exit value.

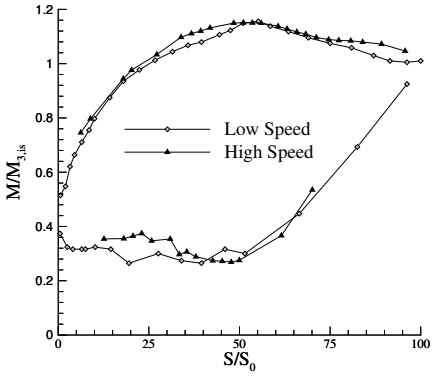

Figure 4. Mach number distribution around the low speed and the high speed profile under steady inflow. $Re_3 = 1.9 \times 10^5$

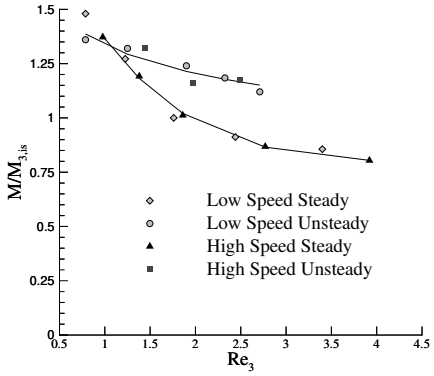

Figure 5. Kinetic Energy (profile) Loss Coefficient KSI versus Reynolds number.

4.2.2 Cascade losses. Pitchwise traverses were performed at midspan behind the high speed and low speed cascade in order to measure the profile loss. Figure 5 shows a plot of the profile losses against Reynolds number for steady and unsteady inflow conditions for both cascades. The design exit Mach number of the high speed blade is 0.64. The kinetic energy loss coefficient KSI is used for the high speed cascade to allow a comparison to be made with the low speed cascade. This is because it is equal to the stagnation pressure loss coefficient when the flow is incompressible. It is seen in the figure that the same trends and the same absolute levels of losses are found for the low speed and high speed cascades. This is true for both steady and unsteady inflow conditions. Figure 5, on its own, answers the question regarding the validity of the low speed approach for the case under consideration.

The LPT blade that both cascades model was designed without considering the effect of unsteady inflow. At $Re_3 = 1.90 \times 10^5$, a small suction side separation bubble features on the blade under steady inflow. When wakes are present, wake induced transition always happens near the separation point. The suppression of this small bubble does not produce any benefit. Instead a penalty occurs because more surface is

covered by turbulent flow thus increasing the losses. At $Re_3 = 0.88 \times 10^5$, the size of the separation bubble increases, being more detrimental in terms of losses. Therefore, the suppression of the separation bubble by the unsteadiness at this condition produces a benefit in terms of losses. The curve of unsteady inflow conditions crosses the one for steady inflow at about $Re_3 = 1.00 \times 10^5$.

4.2.3 Hot films results. Up to this point, the comparison between the high speed and the low speed cascade has been made on the bases of profile loss measurements and Mach number distributions. A comparison of the state of the boundary layer along both profiles is also needed. Multi-element hot film anemometers were used to study the development of the blade surface boundary layer. The description of the technique and the description of the presentation of the data can be extensively found in literature (e.g. Banieghbal et. al, 1995).

The anemometers were fitted at the mid-span of the suction surface of the blade in the central passage Figure 6 and figure 7 present distance-time, ST, diagrams of quasi-shear stress from one of the ensembles of the anemometer data, i.e., raw data. Both figures show data obtained at the design conditions. The same behavior can be identified in both cases. In the results obtained with steady inflow at the design point (not shown here), separation was seen to occur between 75% and 80% of the suction surface. The latter is true for the low speed and the high speed cascade. Figure 6 and 7 show that the onset of transition is moved upstream periodically due to the wake passing effect. Along the wake induced path, the onset of transition occurs near to the point of steady separation (Stieger, 2003). From the onset of transition onwards, the typical wedge shape proper of wake induced transition is seen (Schulte, 1995). This wedge shape is caused by the dissimilar velocity convections of the different characteristic trajectories of the leading and trailing edges of the turbulent spots. Between the wake trajectories, the flow is still separated. Along these paths, transition occurs within the shear layer existing between the free stream and the separation bubble.

4.3 CLT2 Profile

The conclusions drawn in the previous section are valid for a conventional profile. Nowadays, the new profiles tend to have an increased lift coefficient and/or loading in order to reduce either number of blades per stage and/or a full stage of the LPT (Vazquez et al. 2003). These authors argued that lift coefficients higher than 1.2 and mean stage loading parameters higher than 3 were required to achieve a reduction of the

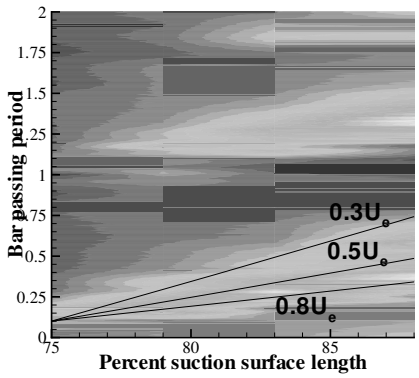

Figure 6. Quasi-shear stress. Design point. Low speed cascade , $Re_3 = 1.9 \times 10^5$, (Banieghbal et al, 1995).

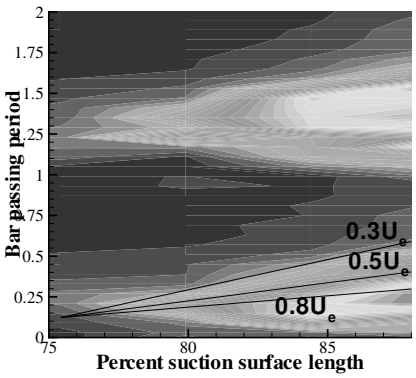

Figure 7. Quasi-shear stress. Design point. High speed cascade. $Re_3 = 1.9 \times 10^5$, $Ma_3 = 0.64$.

number of components of the LPT. With the conventional technology, these new values would lead to an important efficiency penalty associated in part with increased profile losses.

The profile that will be presented next is a blade designed by ITP and it is representative of these new trends. This blade, CLT2, is a high turning profile designed to take account of unsteady inflow conditions. A large suction side separation bubble side occurs on the blade under steady inflow conditions. This bubble is suppressed in the presence of the wakes coming from an upstream blade row during a certain fraction of the wake passing period. Due to compressibility effects, any suppression of a bubble is expected to be more beneficial in high speed flows because of the reduction of blockage. Figure 8 presents the kinetic energy loss coefficient against Mach number under steady and unsteady inflow conditions. The results are shown for the design Reynolds numbers.

For the case under steady inflow, no dependency on Mach number is seen up to $M_3 = 0.76$, from where the losses start to increase. According to Denton (1994), the losses associated with a passage shock wave are generally small unless the shock wave boundary layer interaction produces an earlier separation and therefore, an increase in the losses. For the current case, the first shock waves appear in the passage around $Ma_3 = 0.83$. The increase of losses with Mach number is seen to appear at this Mach number because of the presence of the separation bubble and its increasing size.

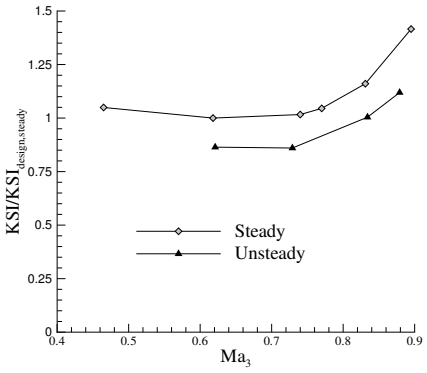

Figure 8. KSI loss coefficient versus Mach number at design Reynolds number (2.0×10^5) for the CLT2 cascade

For the case of unsteady inflow, the losses seem to remain at a constant level at least up to Mach 0.76. The decrease in losses produced by the unsteadiness remains approximately constant for the range of Mach numbers under consideration. It is equivalent to approximately 14% of the steady loss. A benefit is therefore obtained up to $Ma_3 = 0.88$, well within the transonic region.

It should be noticed that these experiments were carried out while keeping constant the rotational speed of the bars. So, the reduced frequency decreases when increasing the Mach number. Therefore, it might be expected that the curve of unsteady inflow conditions approaches that of steady inflow conditions when the Mach number increases. Instead, an approximately constant benefit is obtained for the entire range of Mach numbers under consideration. This is consistent with the suppression of a larger separation bubble at higher Mach numbers but lower reduced frequencies.

5. CONCLUSIONS

The techniques employed in the simulation of unsteadiness in high speed linear cascade testing have been presented and compared to the techniques involved in the low speed tests. Results from a high speed and a low speed cascade, both being models of an existing LPT blade have been compared for steady and unsteady flow conditions. The results have shown that the same quantitative values of losses are obtained, showing the validity of the low speed approach for profiles with an exit Mach number of the order of 0.64.

The previous affirmation has been extended to a high turning profile designed following current design practices. Measurements of the losses have shown that there is no dependency on Mach number up to $Ma_3 = 0.76$. A benefit coming from the wakes is achieved up to an exit Mach number of at least 0.9.

Acknowledgments

The authors would like to thank T. Chandler for his work on the high speed rotating bar rig. The authors would also like to thank ITP, for the funding of the project and the permission to publish this paper.

References

[1] Banieghbal, M.R., Curtis, E.M., Denton, J.D., Hodson, H.P., Huntsman, I., Schulte, V., Harvey, N. W., Steele, A. B., Wake Passing in LP Turbines Blades, presented at the AGARD conference, Derby, UK, May 8-12, 1995

[2] Brunner, S., Fottner, L., Schiffer, H, Comparison of Two Highly Loaded Low Pressure Turbine Cascades under the influence of Wake-Induced Transition ASME 2000-GT-268, 2000

[3] Coton, T.,Arts, T., Lefebvre, M., Liamis, N, Unsteady and calming effects investigation on a very high lift LPT blade, ASME GT-2002-30227, 2002.

[4] Denton, J.D., Loss Mechanism in Turbomachines. IGTI Gas Turbine Scholar Lecture 1994. ASME J Turbomachinery, Oct. 1994.

[5] Doorly, D.J., A Study of the effect of wake passing on Turbine Blades, PhD Thesis, Oxford University, 1984.

[6] Hodson, H.P., Dawes, W.N., On the Interpretation of Measured Profile Losses in Unsteady Wake-Turbine Blade Interaction Studies, 1996.

[7] Hodson, HP, and Dominy, RG, "Annular Cascade Testing", AGARDograph 328 Advanced Methods for Cascade Testing, AGARD, 1993

[8] Schulte, V., Unsteady Separated Boundary Layers in Axial Flow Turbomachinery, PhD Thesis, Cambridge University, 1995.

[9] Schulte, V., Hodson. H.P, Unsteady Wake-Induced Boundary Layer Transition in High Lift LP Turbines, Journal of Turbomachinery, Vol.120, 1996.

[10] Stieger, R.D,, The Effects of Wakes on Separating Boundary Layers in Low Pressure Turbines, PhD Thesis, Cambridge University, 2002.

[11] Vazquez, R., Cadrecha, D., Torre, D., High Stage Loading Low Pressure Turbines. A New Proposal for an Efficiency Chart

[12] Wisler, D.C, Loss Reduction in Axial-Flow Compressors through Low-Speed Model Testing ASME 84-GT-184, 1984.